Supplement of Atmos. Meas. Tech., 19, 3309–3332, 2026
https://doi.org/10.5194/amt-19-3309-2026-supplement


Atmospheric Measurement Techniques
Open Access
EGU

*Supplement of*

# Ground-based total ozone column measurements in the Huggins and Chappuis bands using Direct-Sun DOAS observations

**Dimitris Karagkiozidis et al.**

*Correspondence to:* Dimitris Karagkiozidis (dkaragki@auth.gr)

**S1: Solar irradiance data**

Figure S1 presents the pyranometer measurements of diffuse, global, and direct solar irradiance recorded in Thessaloniki on 6 May 2024 and 21 June 2023. The data from the 6$^{th}$ of May are characterized by stable clear-sky conditions and this day was selected for the definition of the reference spectrum applied in the DOAS analysis. Data from the 21$^{st}$ of June, corresponding to the summer solstice and maximum solar elevation, was used to estimate the ozone SCD of the reference spectrum through the Langley plot method (Sect. 3.4).

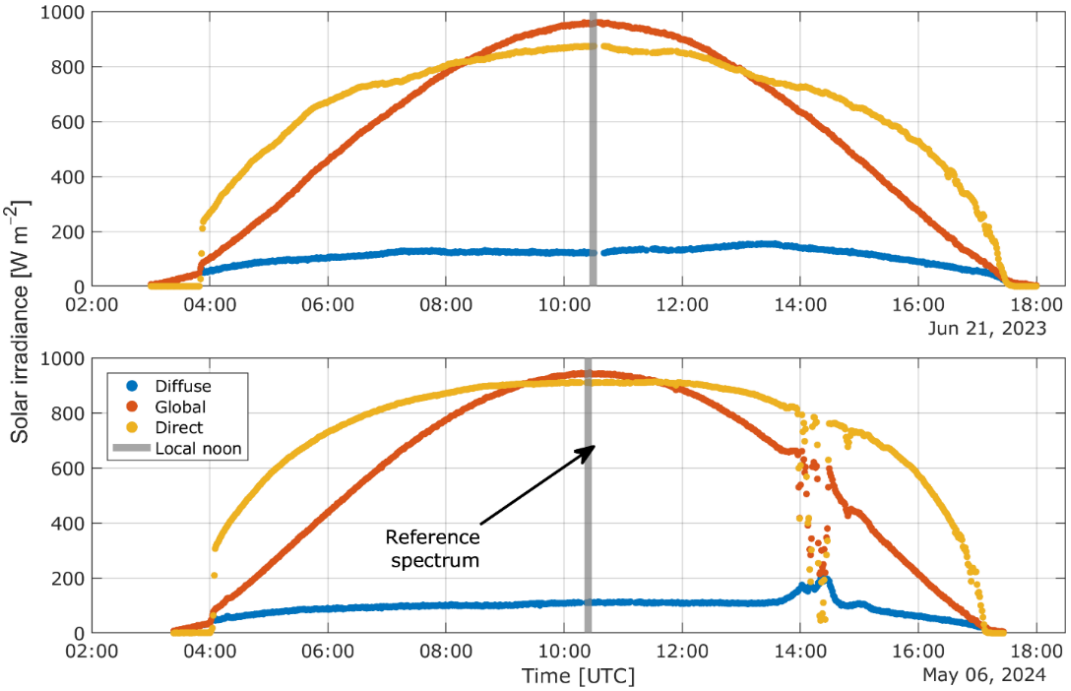


**Figure S1:** Diurnal variability of diffuse (blue), global (orange), and direct (yellow) solar irradiance on 21 June 2023 (top panel) and 6 May 2024 (bottom panel) measured by the pyranometers in Thessaloniki.

**S2: DOAS fit RMS as a function of SZA**

Figure S2 illustrates the dependence of the DOAS fit RMS on SZA for the UV and VIS $O_3$ retrievals. The data are grouped in 5° SZA bins below 80°, and in 1° bins above 80°. Across all bins, the VIS retrievals show consistently lower RMS values than the UV, indicating a higher SNR in the visible spectral range. Although both spectral regions show an increase in RMS with increasing SZA, the UV RMS increases more rapidly above approximately 70°, which is indicative of reduced fitting stability under low solar elevations. In contrast, the VIS RMS remains comparatively stable. It should also be noted that slight differences between the UV and VIS variability may be influenced by the different temporal coverage of the two datasets (see Sect. 2.2), resulting in fewer data at certain SZAs.

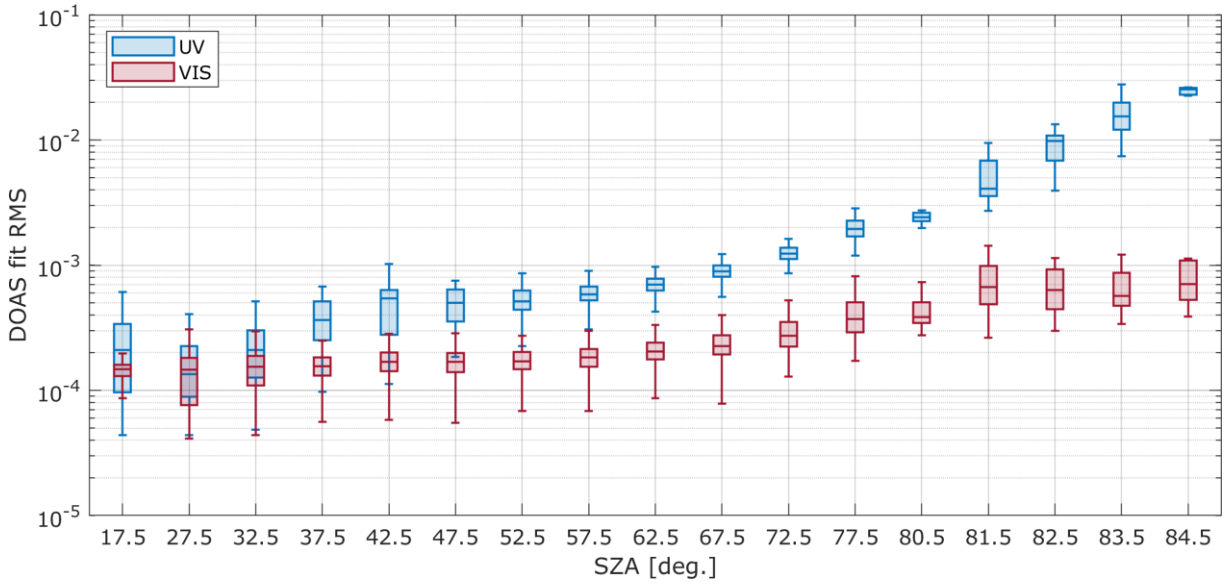


**Figure S2:** Dependence of DOAS fit RMS on SZA for the UV and VIS $O_3$ retrievals.

**S3: Intercomparison of Brewer and Pandora TOC observations**

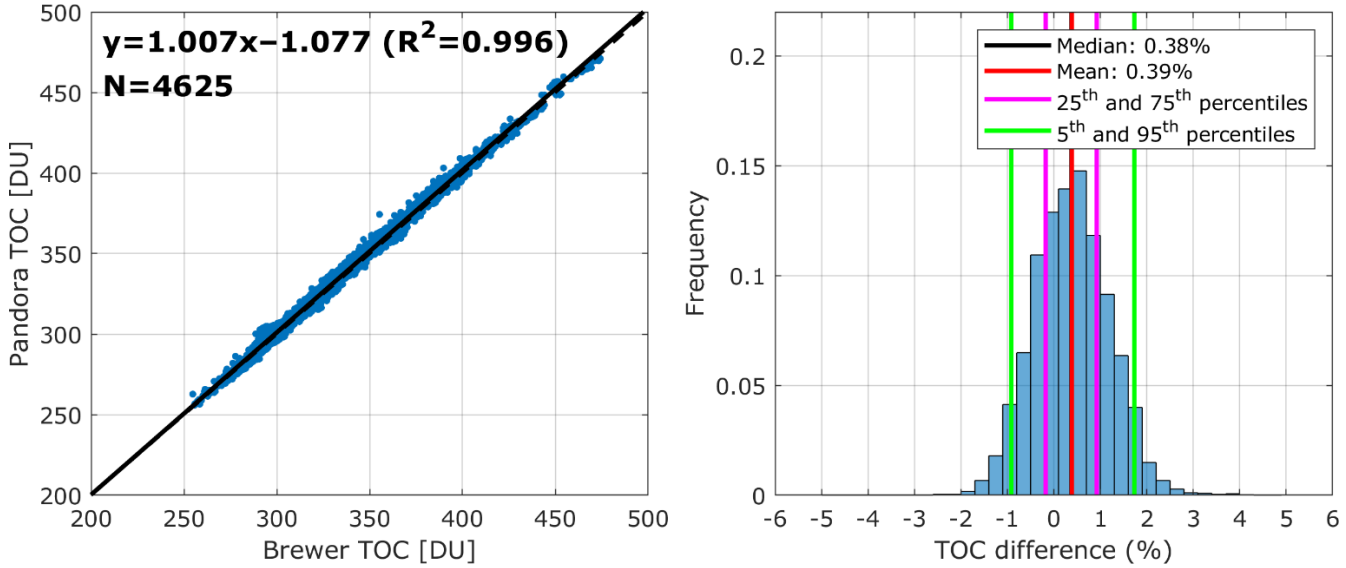


**Figure S3:** Comparison of collocated TOC measurements from Pandora and Brewer over the study period. The left panel shows a scatter plot of the TOC observations, with the regression fit (solid line) and the 1:1 reference (dashed line). N corresponds to the number of collocated measurements. The right panel shows the corresponding frequency distribution of TOC percentage differences (Pandora–Brewer), with mean, median, and percentile ranges indicated.

## S4: The wildfire event of Alexandroupolis

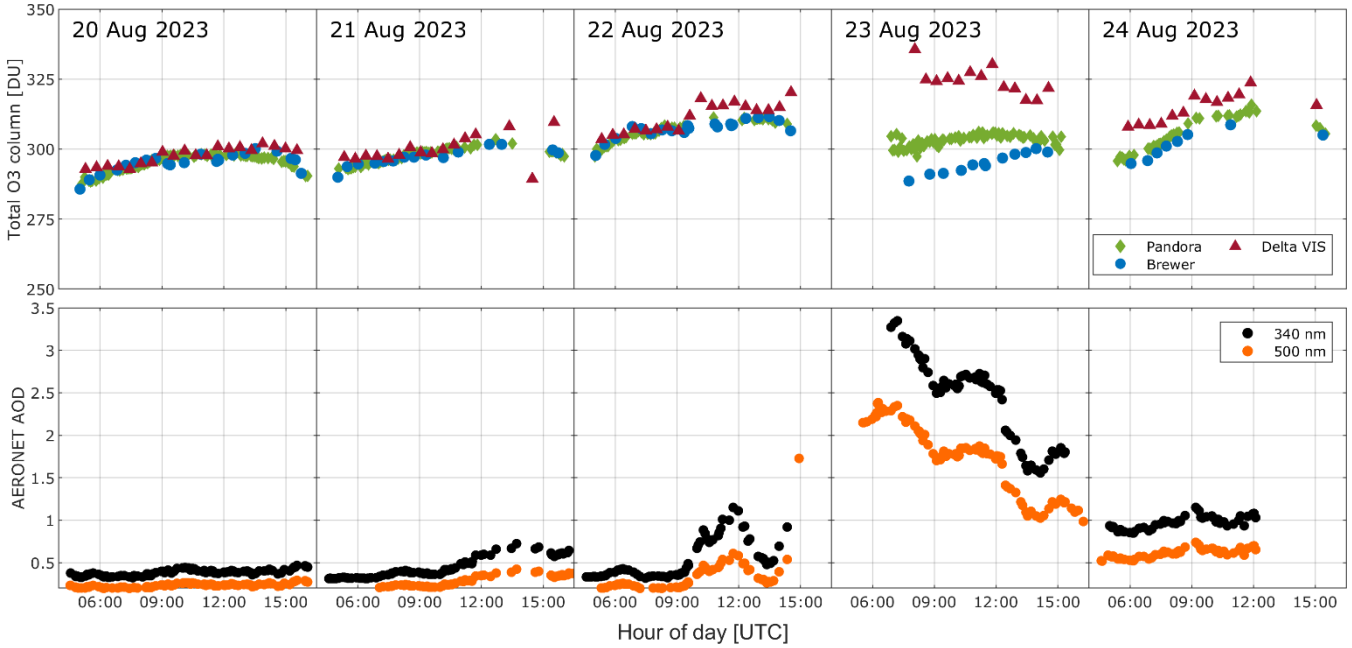


**Figure S4:** Time series of TOC from Pandora, Brewer, and Delta VIS retrievals (top row) and the respective AOD measurements at 340 and 500 nm (bottom row) during the wildfire event of Alexandroupolis in August 2023.

**S5: Intercomparison of TOC diurnal variability**

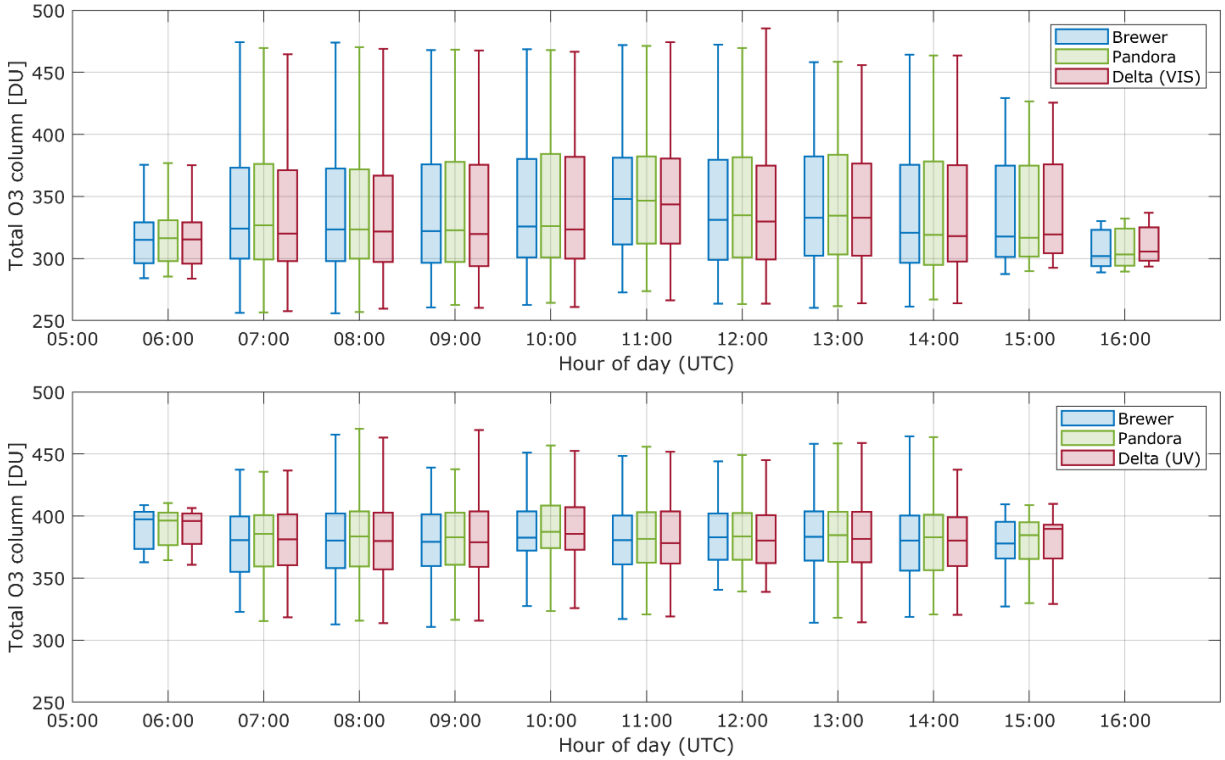


**Figure S5:** Box-and-whisker plots of the diurnal variability of TOC captured by the Brewer (blue), the Pandora (green) and the Delta (red). The top panel represents collocated measurements of all instruments using Delta VIS data, while the bottom panels using Delta UV data.